Mon. Not. R. astr. Soc. (1987) **228,** 671–679

The extended narrow-line region in radio Seyferts: evidence for a collimated nuclear UV field?

S. W. Unger*, A. Pedlar, David J. Axon *University of Manchester, Nuffield Radio Astronomy Laboratories, Jodrell Bank, Macclesfield, Cheshire SK11 9DL*

M. Whittle†, E. J. A. Meurs, M. J. Ward‡ *Institute of Astronomy, Madingley Road, Cambridge CB3 0HA*

Accepted 1987 April 28. Received 1987 March 24

Summary. Long-slit spectra of seven Seyfert galaxies reveal high-excitation ([O III] λ5007/H$\beta \approx 5$) emission-line gas up to 20 kpc from the galactic nuclei. The low velocity dispersion (FWHM$<$45 km s^{-1}) and orderly velocity field, characteristic of normal galactic rotation, suggest that this emission-line region, the *Extended Narrow Line Region* (ENLR), is physically distinct from the classical Narrow Line Region (NLR).

The large physical extent, high excitation and kinematic properties of the ENLR point to it being ambient gas in the disc or halo of the galaxy which is photoionized by the nuclear radiation field.

Despite the disparity in their physical sizes, the ENLR is substantially more extended parallel to the axis of the NLR radio structure than perpendicular to it. We argue that this elongation is due to an anisotropy in the nuclear radiation field whose origin is intimately related to the collimation of the radio ejecta.

1 Introduction

A prerequisite to developing an understanding of the Narrow Line Region (NLR) is a detailed picture of the geometry and velocity field. However, until recently much of our understanding of the physics of the NLR has been based on single-aperture studies of the emission-line ratios and profiles of Seyfert nuclei. Such observations only yield a picture which is an average over the density, velocity and ionization structure of the gas (e.g. Pequignot 1984; Filippenko & Halpern 1984; Whittle 1985).

The discovery of a correlation between the radio power and the luminosity and linewidth of [O III] λ5007 first suggested the idea of a physical relationship between the NLR and the radio

*Present address: Royal Greenwich Observatory, Herstmonceux Castle, Hailsham, East Sussex BN27 1RP.
†Present address: Department of Astronomy, University of Virginia, Box 3818, University Station, Charlottesville, VA22903-0818, USA.
‡Present address: Department of Astronomy FM-20, University of Washington, Seattle, WA 98195, USA.

structure (e.g. de Bruyn & Wilson 1978; Wilson & Willis 1980; Meurs & Wilson 1984), and this was supported by the discovery in many Seyfert galaxies of linear radio sources of comparable scale lengths to the NLR (e.g. Ulvestad, Wilson & Sramek 1981; Unger *et al.* 1986). Recently much more concrete observational evidence in favour of this picture has emerged. First, narrow-band imaging and spectroscopy have shown that in many cases not only are the physical sizes of the radio structure and the line-emitting gas in the NLR comparable, but the line-emitting gas also has a tendency to be elongated in the same direction as the radio ejecta (Wilson & Heckman 1985, and references therein). Secondly, there are a few galaxies in which discrete velocity components seen in the [O III] λ5007 line profile are closely associated with individual radio components as for example in NGC 5929 (Whittle *et al.* 1986).

It is clear that a combination of radio and optical observations has greatly improved our understanding of the NLR. There are a few Seyfert galaxies in which high-excitation gas has been detected at much larger distances from the galactic nucleus than the classical NLR (e.g. NGC 4151: Heckman & Balick 1983), and it is interesting to ask if the radio structure is relevant here. Early observations of NGC 4151 suggested that the extended emission-line region in this object was highly elongated (Simkin 1975) and that deviations of several hundred km s^{-1} from the systemic velocity were present (Fricke & Reinhardt 1974), leading Booler, Pedlar & Davies (1982) to propose that the gas had been ejected from the nucleus. However, some doubt was cast on this suggestion by Heckman *et al.* (1981), who did not confirm the high velocities. In this paper we present long-slit spectra of seven Seyfert galaxies with extended emission-line regions similar to that seen in NGC 4151. We show that the kinematics of the gas is inconsistent with it having been ejected from the nucleus, and put forward an alternative explanation for the observed elongation of the emission-line regions along the radio axis.

2 Observations

Long-slit observations of the galaxies listed in Table 1 were obtained at the $f/15$ Cassegrain focus of the 2.5-m Isaac Newton Telescope using the Intermediate Dispersion Spectrograph and the IPCS detector (Boksenberg 1972; Boksenberg & Burgess 1973). A grating with 1200 lines per mm gave a FWHM instrumental resolution of 0.75 Å (45 km s^{-1}) and a 500 Å range covering Hβ and [O III] λ4959, 5007. A 70 arcsec slit of width 0.63 arcsec contained 112 spatial increments, each of length 0.63 arcsec.

Each galaxy was observed at two orthogonal position angles. For the majority of the galaxies these were chosen to be approximately parallel and perpendicular to the radio axis. In the case of NGC 4151 the slit position angles were oriented relative to the extended emission-line region seen on the narrow-band image by Heckman & Balick (1983). A journal of the observations is given in Table 2. The seeing estimates were derived from the brightness profiles of either photometric standards or the unresolved Hβ broad-line emission where present.

Wavelength calibration using 10–20 Cu–Ar arc lamp lines gave typical residuals of 2–4 km s^{-1}. Observations of standard stars through a wide slit in photometric conditions permitted absolute flux density calibration for all objects except Mkn 573 and NGC 4151. An approximate calibration for NGC 4151 was obtained by comparing our observations with those of Heckman & Balick (1983).

3 Results

Plates 1–4 show grey-scale representations of the observed intensity as a function of wavelength and position along the slit for the spectra listed in Table 2. Although broad velocity structure characteristic of the NLR (FWHM~500 km s^{-1}) is apparent close to the nucleus, the objects we

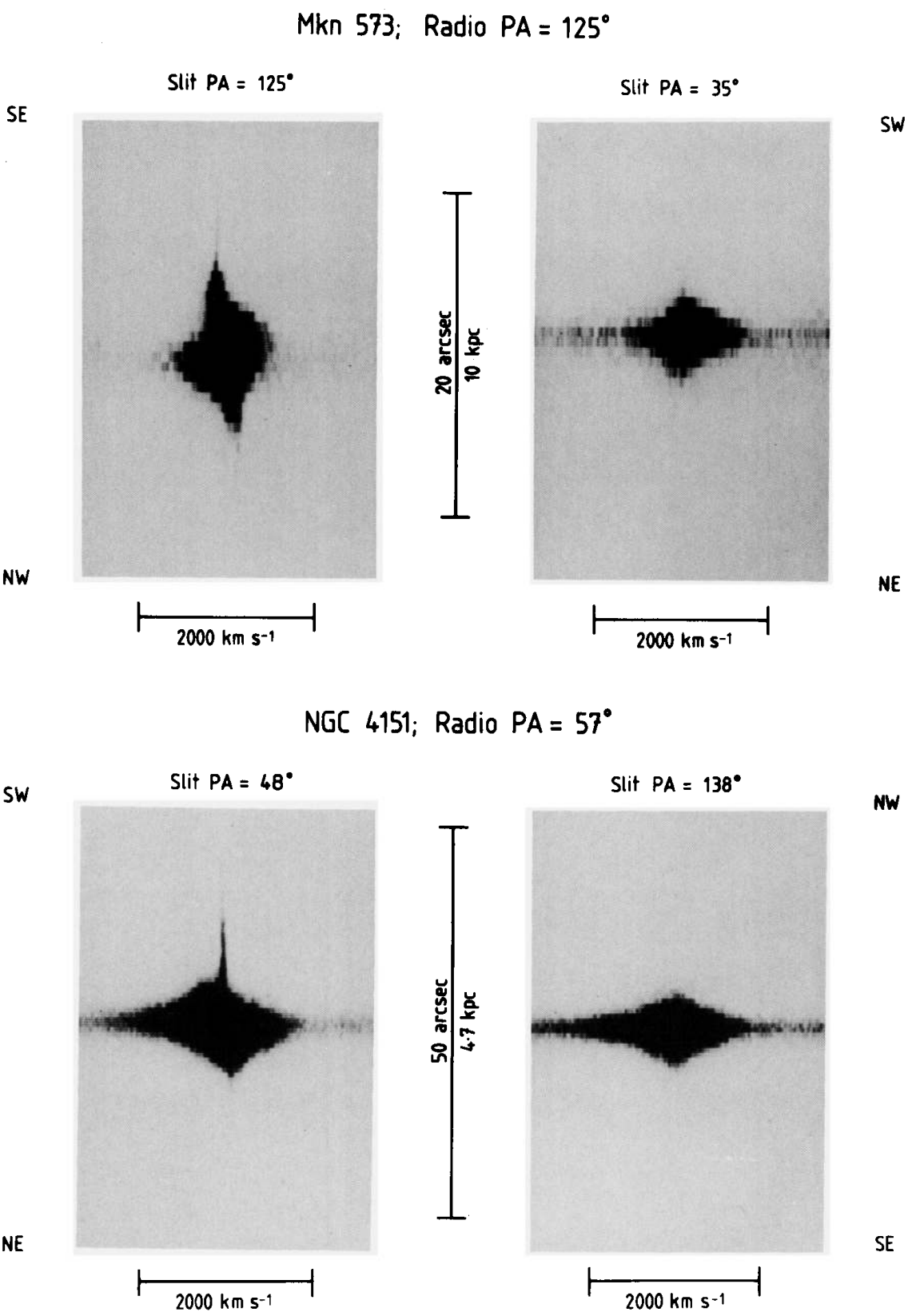

Plate 1

Plates 1–4. Grey-scale representations of long-slit spectra of Mkn 573, NGC 4151, Mkn 78, Mkn 6, NGC 3516, NGC 5252 and Mkn 34. Pairs of objects with similar ENLR morphologies are grouped together. Spectra are presented for each object in two perpendicular PAs. The two spectra for each object have the same intensity scale (in counts s^{-1}), so that a visual inspection can show which spectrum has the more extended line emission. The wavelength range usually includes only the [O III] λ5007 emission line, except for Mkn 6 and Mkn 34 in which the [O III] λ4959 line can also be seen. A bar underneath each spectrum gives the velocity scale, and a vertical bar gives an angular scale in arcsec and the corresponding linear scale in kpc.

[*facing page* 672]

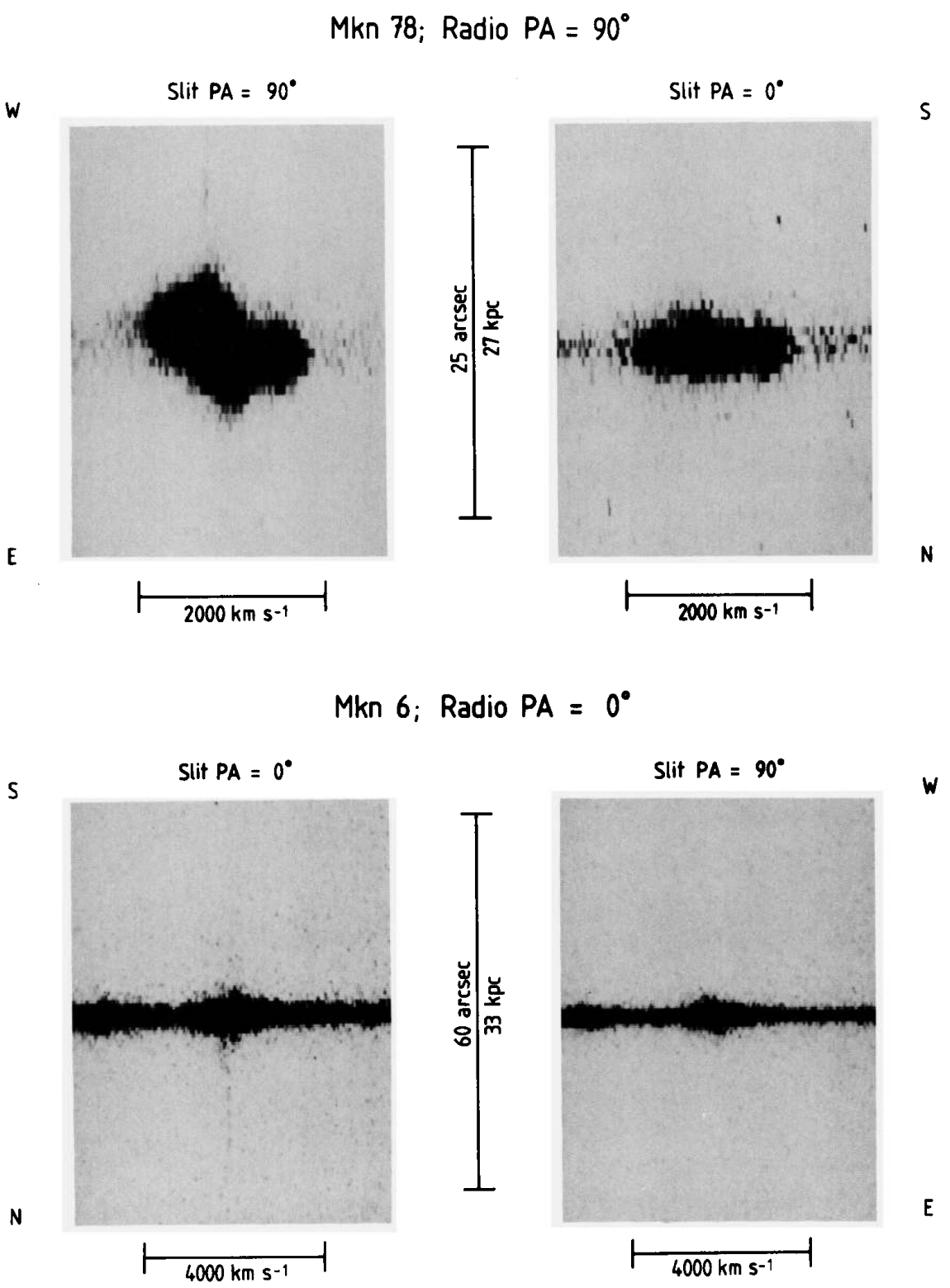

Plate 2

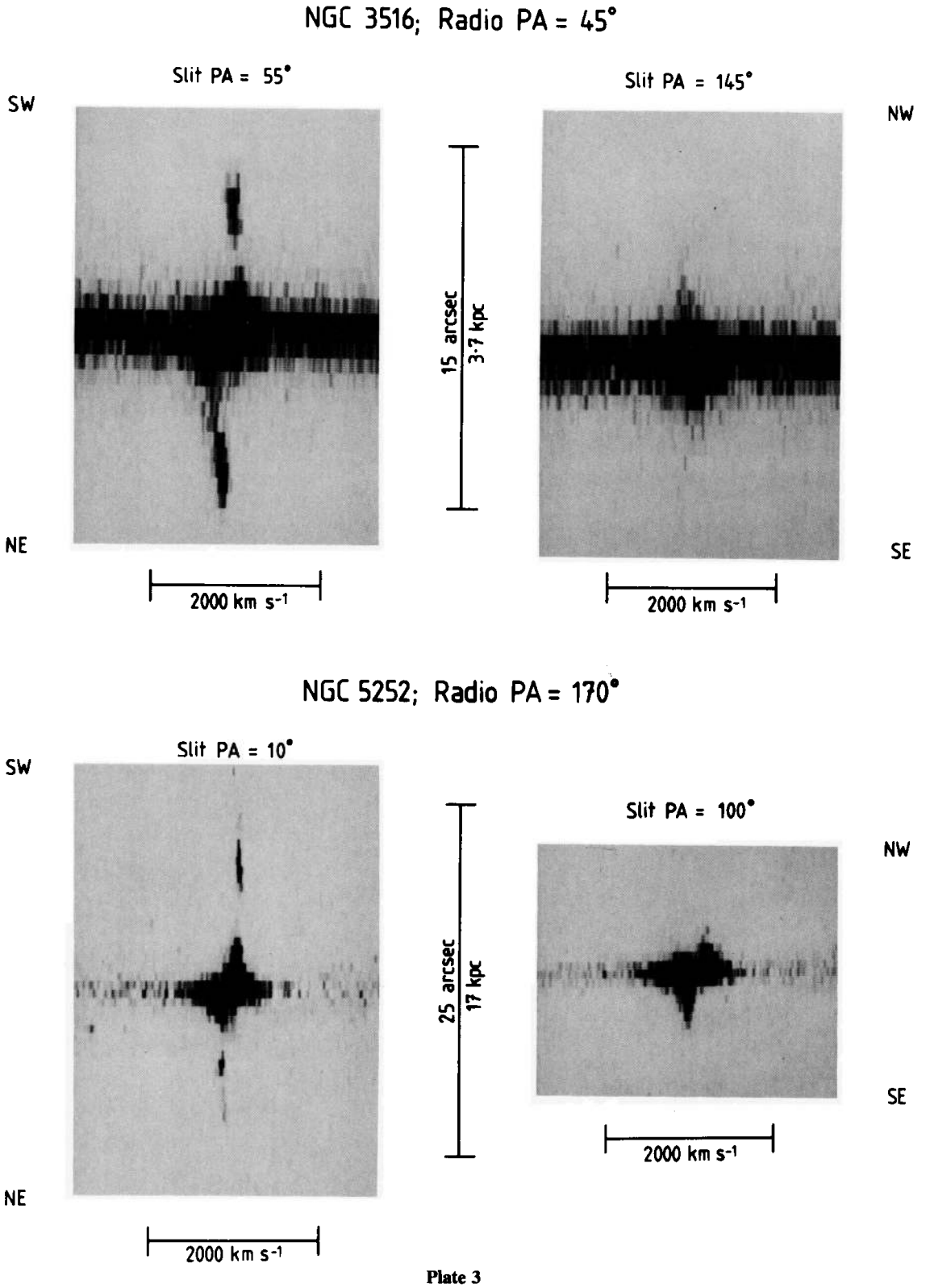

Plate 3

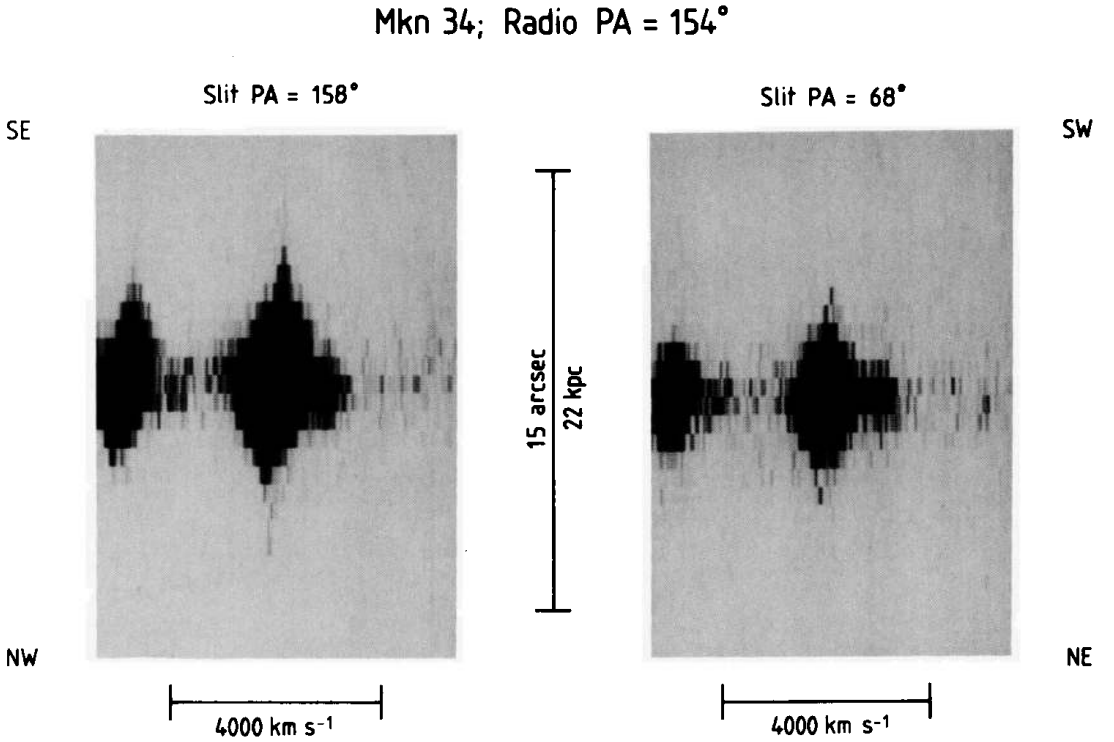

Plate 4

Table 1. Properties of the galaxies observed.

(1)	(2)	(3)	(4)	(5)	(6)	(7)	(8)
Mkn 6	5660	S0a	1.5	0.6	127	0	1,7,9,10
Mkn 34	15355		2	0.64	27	158	1,5,9
Mkn 78	11136		2	0.41	85	90	1,5,9
Mkn 573	5173	S0	2	0.75	~4	125	1,5,6,7,9
NGC 3516	2540	SB0	1	0.75	55	45	2,5,7,9
NGC 4151	970	SBab	1.5	0.74	26	57	3,5,8,9,10
NGC 5252	6926	S0	2	0.63	10	170	4,7,9

Key to columns:
(1) Galaxy.
(2) Heliocentric velocity (km s^{-1}).
(3) Hubble type.
(4) Seyfert type.
(5) Axial ratio of galaxy.
(6) PA of optical major axis of galaxy (degrees).
(7) PA of radio axis (degrees).
(8) References.

Key to references (the numbers in brackets are the columns to which the references refer):
(1) Ulvestad & Wilson 1984 (7).
(2) E. J. A. Meurs, private communication (7).
(3) Harrison *et al.* 1986 (7).
(4) Axon *et al.*, in preparation (3, 7).
(5) Keel 1980 (5).
(6) Estimated from Palomar Sky Survey print (6).
(7) Nilsson 1973 (3, 5, 6).
(8) Davies 1973 (3, 6).
(9) Huchra 1984 (unpublished list of Seyfert galaxies) (2, 4).
(10) Osterbrock & Koski 1976 (4).

Table 2. Observing parameters.

Galaxy	Slit PA (degrees)	Date	Integration time (s)	FWHM of seeing disk (arcsec)
Mkn 6	0	85 Mar 12	1000	1.8
	90	85 Dec 21	1500	1.1
Mkn 34	338	85 Mar 12	1300	1.7
	68	85 Mar 12	1000	1.7
Mkn 78	90	85 Mar 11	2879	1.7
	0	85 Mar 12	1000	1.7
Mkn 573	35	84 Oct 15	4000	1.3
	305	84 Oct 15	3500	1.3
NGC 3516	145	85 Mar 12	500	1.6
	55	85 Mar 12	750	1.6
NGC 4151	48	85 Mar 10	1924	1.7
	138	85 Mar 11	1050	1.7
NGC 5252	10	85 Mar 12	1000	1.6
	100	85 Mar 12	1100	1.6

discuss here have been selected because they also show evidence for a component of high-excitation ([O III] λ5007/H$\beta \approx 5$), yet narrow-linewidth (FWHM typically <45 km s^{-1}) emission extending up to 20 kpc from the nucleus. In this paper we concentrate on the properties of this outer emission which we shall term the 'Extended Narrow Line Region (ENLR)'.

We illustrate the distinction between the NLR and ENLR using the results for Mkn 573. Fig. 1 shows the variation of peak intensity, linewidth and velocity derived from single Gaussian fits to the [O III] λ5007 profile in each spatial increment along the slit in PA=305°. Within ~4 arcsec of the nucleus the emission-line gas has a large linewidth (FWHM of a few hundred km s^{-1}) and high intensity, typical of the NLR. Between ~4 and ~10 arcsec there is [O III] emission with a much lower intensity, unresolved line profile (FWHM<45 km s^{-1}) and small velocity gradient, the ENLR.

It is clear that the ENLR can be separated from the NLR on the basis of both its kinematics and spatial extent. The other important defining characteristic of the ENLR is the high excitation,

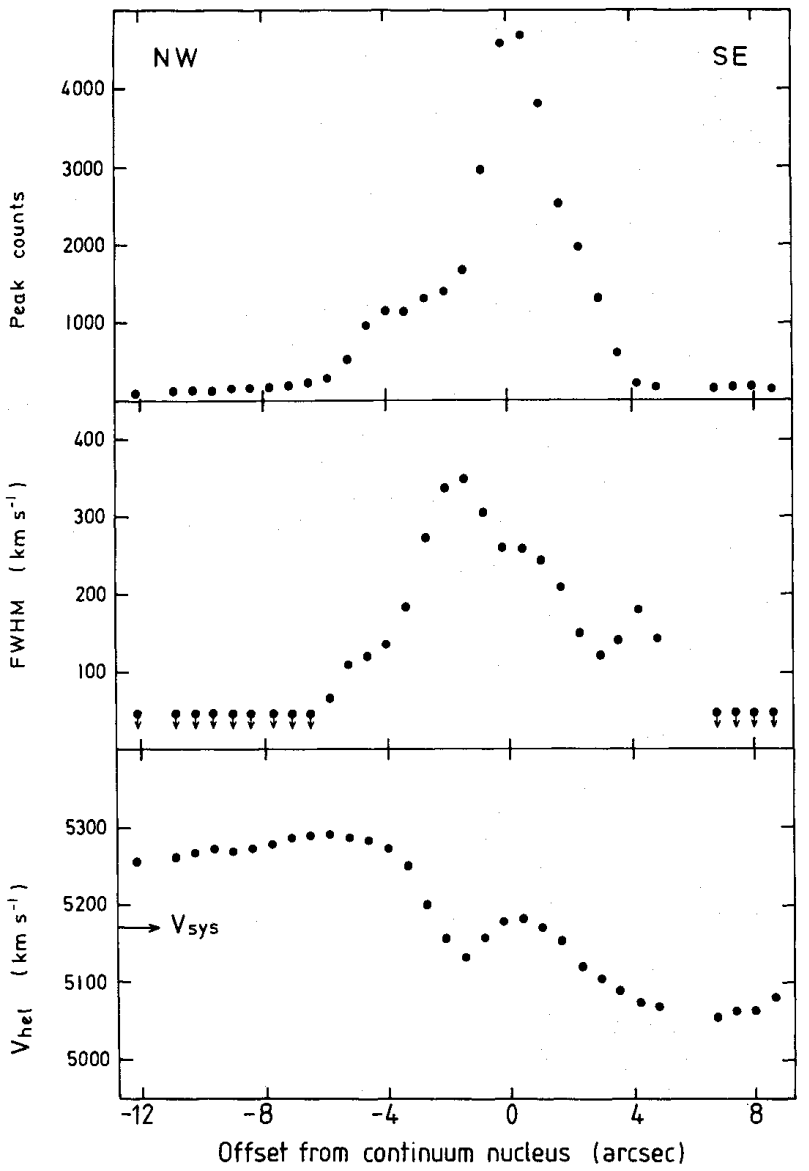

Figure 1. The peak intensity, linewidth and heliocentric velocity of the [O III] λ5007 A emission seen in the long-slit spectrum of Mkn 573 in PA=305°. These parameters have been derived using a single Gaussian fit to the line profile in each spatial increment. The formal errors on the parameters are too small to be represented on this plot.

since this distinguishes the extended emission-line regions discussed in this paper from those associated with extranuclear starbursts (Wilson 1986, and references therein).

Table 3 summarizes some properties of the ENLR emission. Intrinsic parameters are calculated using the redshifts in Table 1 and H_0=50 km s^{-1} Mpc^{-1}. The integrated spectrum of the ENLR on each side of the galactic nucleus was used to derive the peak number of counts in the [O III] λ5007 emission line and the RMS noise level. The mean [O III] λ5007 surface brightness was obtained by dividing the total ENLR flux density measured through the slit by the area of the slit over which the emission was detected. The maximum distance from the nucleus of the ENLR emission has been estimated by eye from Plates 1–4. The heliocentric velocity of the summed [O III] λ5007 emission was measured using a Gaussian fit to the profile. The velocity gradient across the ENLR is usually small (see Fig. 1), and so the velocity of the gas in individual spatial increments is unlikely to differ by more than $\approx$50 km s^{-1} from this average value. Finally, we give an estimate of the line ratio F([O III] λ5007)/F(Hβ) (henceforth 5007/Hβ). The uncertainty in

Table 3. Observed properties of the ENLR.

(1)	(2)	(3)	(4)	(5)	(6)	(7)	(8)
Mkn 6	N	25	4.5	-16.0	19	5582±19	>1.5
	S	<14	4.7				
Mkn 34	NW	17	1.7	-15.3	12	15135±13	>2
	SE	18	1.8	-15.3	12	15419±13	>3
Mkn 78	W	69	4.4	-15.6	16	10916±5	4 ± 1.5
	E	<15	5.2				
Mkn 573	NW	146	5.5		6.1	5279±5	6 ± 2
	SE	36	3.4		4.4	5064±5	>3
NGC 3516	NE	86	2.3	-14.2	1.7	2571±5	6 ± 1
	SW	67	2.8	-14.4	1.3	2656±5	5 ± 1
NGC 4151	NE	91	7.1	-13.6	1.8	1067±5	>2.5
	SW	1393	11.2	-13.0	2.0	955±5	9.2± 0.3
NGC 5252	NE	43	2.7	-15.1	6.2	6823±6	>2
	SW	108	3.6	-15.1	11	7004±5	6.5± 1.5

Key to columns:
(1) Galaxy.
(2) ENLR component.
(3) Peak of [O III] λ5007 for integrated spectrum (counts). Upper limits are three times the RMS noise given in column 4.
(4) RMS noise level in the continuum for integrated spectrum (counts).
(5) Log [O III] λ5007 surface brightness (erg s^{-1} cm^{-2} $arcsec^{-2}$).
(6) Maximum distance from nucleus of detected ENLR emission (kpc).
(7) Heliocentric velocity of [O III] λ5007 (km s^{-1}).
(8) Line ratio F([O III] λ5007)/F(Hβ).

this parameter is large, since the Hβ line is often very weak and may also be influenced by underlying stellar absorption.

4 Observed properties of the ENLR

4.1 SPATIAL DISTRIBUTION

Inspection of Plates 1–4 clearly shows that for each galaxy the ENLR emission is visible in only one of the two orthogonal slit position angles, implying that the emission is highly elongated. Note that although the integration times for the two slit positions on each object are not equal, the signal-to-noise ratio for the detected ENLR emission (see columns 3 and 4 of Table 3) is always sufficiently high that emission would be detected in the other slit spectrum if it were present with the same intensity. The highly elongated nature of the ENLR is confirmed for NGC 4151 by a narrow-band [O III] λ5007 image (Heckman & Balick 1983), which shows most of the emission to lie in a wedge of opening angle 10°.

Where ENLR emission is seen on both sides of the nucleus, the intensity ratio ranges between 1:1 and 14:1 (see column 3 of Table 3). The two objects for which the ENLR emission appears to be one-sided (Mkn 6 and 78) are not necessarily any more asymmetric than the other objects, but just fainter (intensity ratios >2 and >4, respectively).

All of the objects in our sample except NGC 4151 have an unambiguous radio axis. In all these cases the ENLR emission has a greater extent parallel to the radio axis than perpendicular to it (see Plates 1–4). In NGC 4151 the radio axis changes significantly from PA=57° on an angular scale of 20 marcsec to PA=83° on an angular scale of $\geq$0.5 arcsec (Harrison *et al.* 1986). The ENLR emission is extended in PA=48° (*cf.* Heckman & Balick 1983), close to the *inner* radio axis.

Despite the elongation of the ENLR emission close to the radio axis, there is no direct spatial association between the radio source and line-emitting gas. In particular, the ENLR emission

usually has a much greater extent (up to 20 kpc) than the radio emission, which in all the objects except NGC 3516 and NGC 5252 is confined to the classical NLR (extent≈1 kpc).

4.2 EMISSION-LINE RATIOS

For the objects in which Hβ can be detected, the 5007/Hβ ratio lies in the range 4 to 9, whilst for the fainter objects we obtain lower limits to the ratio of 1–3. This implies that the ENLR has an intermediate excitation between that of normal H II regions (5007/Hβ≈0.1–1) and the classical NLR (5007/Hβ≈10) (Baldwin, Phillips & Terlevich 1981). For example, although the ENLR in NGC 4151 has the highest excitation in our sample (5007/Hβ=9.2), this is still less than that of the NLR (5007/Hβ=16; Boksenberg *et al.* 1975).

4.3 KINEMATICS

In contrast to the NLR emission which has relatively broad (FWHM~300–500 km s^{-1}) lines showing considerable substructure, the ENLR emission has extremely narrow lines. In the brighter objects such as NGC 4151 or Mkn 573, where it is possible to measure the linewidth of gas in individual spatial increments, the lines are generally unresolved with FWHM<45 km s^{-1}. This is comparable with the velocity dispersion of 7–10 km s^{-1} for neutral gas (van der Kruit & Shostak 1984) and of ≈20 km s^{-1} for H II regions in the discs of normal spiral galaxies.

The orderly, slowly-varying velocity field suggests that the gas is undergoing normal galactic rotation, with the emission originating principally on the flat part of the rotation curve. For objects in which ENLR emission is seen on both sides of the nucleus, this suggestion is supported by the magnitude of the velocity difference between the two ENLR components, which gives an estimate of the rotation amplitude along the slit PA. The values of 284, 215, 85, 112 and 181 km s^{-1} for Mkn 34, Mkn 573, NGC 3516, NGC 4151 and NGC 5252, respectively are typical of the rotational velocities of gas in the discs of normal spiral galaxies. For NGC 4151 and NGC 5252, the ENLR velocity differences are less than or equal to the H I linewidths of 153 and 189 km s^{-1}, respectively (Davies 1973; Axon *et al.*, in preparation), as would be expected given that the long-slit spectra are not necessarily aligned with the kinematic major axis of the Galaxy.

5 The ionization of the ENLR gas

Although the velocity field of the ENLR is consistent with rotation in a galactic disc, it seems unlikely that the emission originates from normal H II regions. First, as described above the ENLR emission is highly elongated and preferentially aligned with the radio axis. Since the galaxies do not appear edge-on optically (see column 5 of Table 1), and furthermore the radio axis is not in general aligned with the galactic major axis (see columns 6 and 7 of Table 1), the ENLR gas must have a very different distribution from the disc gas. Secondly, the excitation diagnostic 5007/Hβ is too high to be consistent with normal disc H II regions (see Section 4.2).

Extreme starburst models may avoid the second of these problems since very young and massive star clusters could reproduce the observed 5007/Hβ values (*cf.* Terlevich & Melnick 1985). In this case, the coincidence between the ENLR and radio position angles might be explained by star formation triggered by jet interaction with the ambient medium, similar to that found in NGC 541 (van Breugel *et al.* 1985). One problem with this view, however, is that the ENLR lies well beyond the observed radio structure. The interaction and resulting star formation might be expected to produce detectable radio emission throughout the ENLR as well as significant velocity perturbation, neither of which is observed.

One obvious source of ionizing radiation is the nuclear continuum source, thought to be

responsible for ionizing the broad- and narrow-line region material. Once again, an important constraint for this picture is the observed elongation of the ENLR close to the radio axis. If the nuclear UV field is isotropic, this implies that the gas in the galaxy must also be highly elongated parallel to the radio axis (see Section 4.1). The only obvious way in which such a peculiar gas distribution might arise is if gas is ejected or pushed away from the nucleus by a kiloparsec-scale radio jet. However, the observed linewidth and the velocity field of the gas are inconsistent with turbulent outflow (see Section 4.3).

If the distribution of gas in the galaxy is *not* highly elongated, then we have the important result that the ionizing UV field must be highly anisotropic, with UV photons preferentially escaping from the nucleus along the radio axis (see also Osterbrock 1984; Morris *et al.* 1985).

We can test whether this interpretation is energetically feasible by estimating the ionizing flux from the optical non-thermal continuum luminosities given by Yee (1980), assuming a continuum distribution of the form $S_\nu \propto \nu^{-1}$. The anisotropy of the UV field renders this a lower limit to the ionizing radiation emitted in the direction of the ENLR. A comparison with the surface brightnesses listed in Table 3 then shows that there is, in fact, sufficient radiation to photoionize the ENLR gas.

If the UV field is indeed collimated, how and where does the collimation occur? One possibility is that the radio axis is aligned with the symmetry axis of an optically thick torus which shadows most of the UV flux. There are a number of ways in which this geometry could arise: (i) the radio source is directly collimated by the torus, (ii) the ejection of radio plasma destroys obscuring material along the radio axis, (iii) the radio axis is determined by the angular momentum vector of the torus, as might be expected if the torus were responsible for fuelling a central engine. Note that the PA of the optical continuum polarization in Seyfert galaxies is known to be related to the radio PA (Antonucci 1983), supporting our suggestion that the distribution of material is indeed related to the radio structure.

In NGC 4151 the ENLR is aligned with the innermost radio axis, which refers to an angular scale of $\approx$20 mas ($\approx$2 pc), and *not* with the larger scale radio structure (>0.5 arcsec; >50 pc). This suggests that the scale on which collimation occurs is <1 pc for this object. Since most of the objects displaying ENLR emission are Seyfert 2 galaxies, the collimation is unlikely to be associated with a visible broad-line region, but rather with the inner parts of the NLR or possibly a region close to the central engine itself.

6 Implications of an anisotropic ionizing source

(i) If collimation of the ionizing radiation occurs interior to the NLR, then line emission in the NLR may also be elongated along the radio axis. Note that the suggestion that the radio structure and NLR emission morphology are related via a common collimation process is distinct from the model of Pedlar, Dyson & Unger (1985), in which expanding radio components produce enhanced line emission more directly by compressing the ambient gas. In practice both effects might be important (see fig. 4 of Pedlar *et al.* 1986).

(ii) Our picture of the ENLR requires at least some ionizing radiation to penetrate the NLR to ionize the ENLR gas. The NLR must therefore have a covering factor <1, at least along the directions in which ENLR emission is seen.

(iii) The ENLR in some of the galaxies observed is seen at projected distances of up to 20 kpc from the nuclei, much greater than the scale height of a normal galactic disc. If the ENLR is, in fact, confined to the galactic disc then the collimating axis for the ionizing radiation and, by association, the radio axis must also lie in the plane of the galaxy. The orientation of the radio axis with respect to the disc has been difficult to ascertain and arguments based on the geometry of the ENLR may help. If, on the other hand, the ENLR is *not* confined to the galactic plane we must

infer the presence of a significant amount of gas at a vertical distance of up to 20 kpc from the galactic plane. If the latter is the case then the ENLR may be similar in kind to the very extended emission-line regions seen several tens of kiloparsecs from the nuclei of elliptical radio galaxies such as PKS 0634−20 (Fosbury *et al.* 1984), and may also be related to the optical 'fuzz' seen to surround some quasars (e.g. Bergeron *et al.* 1983).

7 Further work

It is important to determine whether ENLR emission is present in all Seyfert galaxies, or whether it occurs preferentially in particular galaxy types. This requires a deeper search of more objects.

Our present observations only sample two orthogonal slit position angles, preventing a detailed analysis of the ENLR morphology. Two-dimensional mapping is required to determine how elongated the ENLR emission is and how closely the ENLR is aligned with the radio axis. If our interpretation of the ENLR is correct, then the observed spatial distribution of the ENLR gas provides indirect information on the polar diagram of the nuclear UV field.

Acknowledgments

We are grateful to the staff at the INT for assistance with the observations, Brian Harrison for reducing the spectra of NGC 4151, and Ron Ekers and Mike Penston for useful comments. EJAM is supported by an ESA Research Fellowship, MJW by an SERC Advanced Fellowship and MW by a Research Fellowship from Jesus College. The Isaac Newton Telescope, on the island of La Palma, is operated by the Royal Greenwich Observatory at the Spanish Observatorio del Roque de los Muchachos of the Instituto de Astrofisica de Canarias.

References

Antonucci, R. R. J., 1983. *Nature,* **303,** 158.
Baldwin, J. A., Phillips, M. M. & Terlevich, R., 1981. *Publs astr. Soc. Pacif.,* **93,** 5.
Bergeron, J., Boksenberg, A., Dennefeld, M. & Tarenghi, M., 1983. *Mon. Not. R. astr. Soc.,* **202,** 125.
Boksenberg, A., 1972. *Auxiliary Instrumentation for Large Telescopes, Proc. ESO–CERN Conf.,* p. 295, eds Lausten, S. & Reiz, A., Geneva.
Boksenberg, A. & Burgess, A., 1973. *Astronomical Observations with Television Sensors,* p. 21, eds Glaspey, J. W. & Walker, G. A. H., Vancouver.
Boksenberg, A., Shortridge, K., Allen, D. A., Fosbury, R. A. E., Penston, M. V. & Savage, A., 1975. *Mon. Not. R. astr. Soc.,* **173,** 381.
Booler, R. V., Pedlar, A. & Davies, R. D., 1982. *Mon. Not. R. astr. Soc.,* **199,** 229.
Davies, R. D., 1973. *Mon. Not. R. astr. Soc.,* **161,** 25P.
de Bruyn, A. G. & Wilson, A. S., 1978. *Astr. Astrophys.,* **64,** 433.
Filippenko, A. V. & Halpern, J. P., 1984. *Astrophys. J.,* **285,** 458.
Fosbury, R. A. E., Tadhunter, C. N., Bland, J. & Danziger, I. J., 1984. *Mon. Not. R. astr. Soc.,* **208,** 955.
Fricke, K. J. & Reinhardt, M., 1974. *Astr. Astrophys.,* **37,** 349.
Harrison, B., Pedlar, A., Unger, S. W., Burgess, P., Graham, D. A. & Preuss, E., 1986. *Mon. Not. R. astr. Soc.,* **218,** 775.
Heckman, T. M. & Balick, B., 1983. *Astrophys. J.,* **268,** 102.
Heckman, T. M., Miley, G. K., van Breugel, W. J. M. & Butcher, H. R., 1981. *Astrophys. J.,* **247,** 403.
Keel, W. C., 1980. *Astr. J.,* **85,** 198.
Meurs, E. J. A. & Wilson, A. S., 1984. *Astr. Astrophys. J.,* **136,** 206.
Morris, S., Ward, M., Whittle, M., Wilson, A. S. & Taylor, K., 1985. *Mon. Not. R. astr. Soc.,* **216,** 193.
Nilsson, P., 1973. *Uppsala General Catalogue of Galaxies,* Uppsala Astronomical Observatory.
Osterbrock, D. E., 1984. *Q. Jl R. astr. Soc.,* **25,** 1.
Osterbrock, D. E. & Kosti, A. T., 1976. *Mon. Not. R. astr. Soc.,* **176,** 61P.
Pedlar, A., Dyson, J. E. & Unger, S. W., 1985. *Mon. Not. R. astr. Soc.,* **214,** 463.

Pedlar, A., Unger, S. W., Dyson, J. E. & Meaburn, J., 1986. In: *Cosmical Gas Dynamics,* p. 65, ed. Kahn, F. D., VNU Science Press.
Pequignot, D., 1984. *Astr. Astrophys.,* **131,** 159.
Simkin, S. M., 1975. *Astrophys. J.,* **200,** 567.
Terlevich, R. & Melnick, J., 1985. *Mon. Not. R. astr. Soc.,* **213,** 841.
Ulvestad, J. S., Wilson, A. S. & Sramek, R. A., 1981. *Astrophys. J.,* **247,** 419.
Ulvestad, J. S. & Wilson, A. S., 1984. *Astrophys. J.,* **285,** 439.
Unger, S. W., Pedlar, A., Booler, R. V. & Harrison, B. A., 1986. *Mon. Not. R. astr. Soc.,* **219,** 387.
van Breugel, W., Filippenko, A. V., Heckman, T. & Miley, G., 1985. *Astrophys. J.,* **293,** 83.
van der Kruit, P. C. & Shostak, G. S., 1984. *Astr. Astrophys.,* **134,** 258.
Whittle, M., 1985. *Mon. Not. R. astr. Soc.,* **213,** 33.
Whittle, M., Haniff, C. A., Ward, M. J., Meurs, E. J. A., Pedlar, A., Unger, S. W., Axon, D. J. & Harrison, B. A., 1986. *Mon. Not. R. astr. Soc.,* **222,** 189.
Wilson, A. S., 1986. *Conf. Star Formation in Galaxies,* Caltech, June 16–19, in press.
Wilson, A. S. & Heckman, T. M., 1985. In: *Astrophysics of Active Galaxies and Quasi-stellar Objects,* p. 39, ed. Miller, J. S., Oxford University Press.
Wilson, A. S. & Willis, A., 1980. *Astrophys. J.,* **240,** 420.
Yee, H. K. C., 1980. *Astrophys. J.,* **241,** 894.